NASA Technical Memorandum 79094

(NASA-TM-79094) TUNGSTEN FIBER REINFORCED FeCrAlY: A FIRST GENERATION COMPOSITE TURBINE BLADE MATERIAL (NASA) 27 p HC A03/MF A01 CSCL 11D

N79-20187

Unclas

G3/24 17061

TUNGSTEN FIBER REINFORCED FeCrAlY - A FIRST GENERATION COMPOSITE TURBINE BLADE MATERIAL

D. W. Petrasek, E. A. Winsa,
L. J. Westfall, and R. A. Signorelli
Lewis Research Center
Cleveland, Ohio

TECHNICAL PAPER to be presented at the
One-hundred eighth Annual Meeting of the
American Institute of Mining, Metallurgical and Petroleum Engineers
New Orleans, Louisiana, February 18-22, 1979

TUNGSTEN FIBER REINFORCED FeCrAlY - A FIRST GENERATION COMPOSITE TURBINE BLADE MATERIAL

by D. W. Petrasek, E. A. Winsa,
L. J. Westfall, and R. A. Signorelli

SUMMARY

Tungsten fiber reinforced superalloys (TFRS) are potentially useful as turbine blade materials because of their high strength. The purpose of the present work was to identify a specific TFRS having the desired combination of other material properties needed in turbine blades in addition to strength. In addition, fabrication and design concepts were developed to demonstrate the feasbility of fabricating a hollow TFRS turbine blade at reasonable cost.

Tungsten-fiber/FeCrAlY was identified as a promising first generation turbine blade material because of the excellent combination of complementary properties possible with this combination of fiber and matrix. The matrix provides a high melting point, low density, excellent oxidation and hot corrosion resistance, limited fiber-matrix interdiffusion at proposed blade temperatures, and excellent ductility to aid in thermal fatigue resistance. The fiber provides high stress-rupture, creep, fatigue, and impact strength together with high thermal conductivity. Property determinations reported on this material indicate that it has adequate properties for turbine blade use, and its use could permit turbine blade operating temperatures over 50 K greater than those of current DS superalloy blades.

Blade fabrication concepts were developed to demonstrate the feasbility of fabricating a hollow W/FeCrAlY turbine blade at reasonable cost. A fabrication cost study reported that a W/FeCrAlY first stage JT9D blade should cost no more than the current directionally solidified superalloy blade. The fabrication concepts assumed in the cost analysis were incorporated into the design of a first stage JT9D composite turbine blade having a potential 50 K use-temperature advantage over the current blade.

INTRODUCTION

Improvement of aircraft gas turbine engine performance and durability would be greatly facilitated by the development of higher strength turbine blade materials. The strength required of turbine blade materials has increased nearly 30 percent during the last 5 years (ref. 1). Even higher strengths will be needed in the future. However, the current blade materials (nickel and cobalt base superalloys) are already being used at 0.8 of their homologous melting points; therefore, substantial improvement of these materials seems unlikely. Fortunately, refractory fiber reinforced superalloy composites may provide the needed strength improvements.

Tungsten fiber reinforced superalloy composites (TFRS) have demonstrated laboratory stress-rupture strengths exceeding those of the best superalloys. Potential 1000-hour stress-rupture strength of 345 MPa at 1370 K has been reported (ref. 2). Corrected for density, this indicates a 165 K use temperature increase over strong superalloys such as Mar M200. Other properties also look promising; for instance, Charpy impact strength of 39 J at 1370 K has been reported (ref. 3).

A turbine blade material needs a combination of properties in addition to strength and impact resistance. Among these are oxidation resistance, thermal fatigue resistance, mechanical fatigue resistance, and fabricability. Although TFRS have been investigated at many laboratories (refs. 2 to 9), no one specific composite composition had been identified as having all of the combination of properties needed. Recently, NASA decided to study fabrication of TFRS turbine blades, and a TFRS was selected for that effort based on available mechanical and physical property data.

The purpose of the work reported herein was the following: First, identify the specific TFRS having the best combination of properties needed for current aircraft engine turbine blade application. Second, demonstrate fabrication and design concepts needed to produce hollow TFRS turbine blades. Third, identify the fabrication costs of TFRS blades relative to conventional blades.

GENERAL TURBINE BLADE MATERIAL REQUIREMENTS

In this section, turbine blade material property requirements will be related to turbine blade operating conditions. The primary requirements are adequate creep-rupture strength, oxidation resistance, thermal and mechanical fatigue resistance, and impact damage resistance.

Creep-rupture life is a function of stress and temperature; hence, consideration of the stress and temperature distributions along the blade airfoil span will indicate the airfoil creep-rupture requirements. Typical distributions are shown schematically in figure 1. At the airfoil tip, centrifugal stresses are very low and temperatures are high; whereas, at the airfoil base, centrifugal stresses are very high and temperature is low. Neither the tip nor base stress-temperature condition is normally life limiting (this is indicated by the creep-rupture life plot on figure 1). However, near the middle of the airfoil span there is a zone where the combination of stress and temperature results in the shortest computed life. It is the creep-rupture life of this critical zone for failure that limits the airfoil life. The actual stress and temperature in the critical zone are a function of engine design. While a nominal figure for stress in this zone might be 150 MPa, stresses can be as low as 80 MPa in some engines and as high as 240 MPa in others. (These are for 1000-hour lifetimes and 8500 kg/m^3 material density). The metal temperature in this zone can range from 1070 to 1370 K; the temperature is limited by airfoil stresses and material strength. Operating temperature improvements are much sought after. An improvement of 50 K over current alloys is considered significant.

Such an improvement could be used to increase engine operating temperature, lower engine cooling requirements, or increase engine durability.

Creep-rupture strength is also important in the blade root. Stresses in the dovetail attachment region (where the blade is attached to the disk) can be high enough to limit blade life, even though temperatures are only 800 to 1100 K. Localized stresses as high as 700 MPa have been calculated to exist in this region in highly stressed blades (ref. 10).

Thermal fatigue is also a life limiting factor. High transient thermal gradients are produced during engine starts, shut downs, and power setting changes. These gradients cause temporarily high stresses, especially at the airfoil leading edge and at cooling holes. Thus, adequate thermal fatigue resistance is a major requirement.

Oxidation-sulfidation corrosion can also limit life, particularly in blades designed for use at the highest temperatures. Oxygen partial pressures of 2 to 4 atmospheres are present in the turbine. Moreover, sulfur (from the fuel) and alkali salts (ingested with intake air) are present. These can cause accelerated oxidation with sulfide formation commonly referred to as hot corrosion. Thus, good oxidation and hot corrosion properties are another key requirement of turbine blade materials.

Mechanical fatigue can limit blade life. Engine starts, shut downs, and power changes result in changes in centrifugal and gas load forces. These changes can induce low cycle fatigue (LCF) failures. Changes in gas pressure around the combustor ring can cause blade vibrations as can engine unbalance. These vibrations, in turn, can induce high cycle fatigue (HCF) failures. As a consequence, good mechanical fatigue resistance (both LCF and HCF) is required of blade materials.

Lastly, the blades are subject to random impact loadings during maintenance and operation. The blade must be tough enough to withstand this form of abuse.

COMPOSITE TURBINE BLADE MATERIAL REQUIREMENTS

Any TFRS composition selected as a serious blade material candidate must have a combination of the previously mentioned properties if it is to achieve a 50 K advantage over the best current alloys.

The properties of the composite are functions of the fiber and matrix properties. Therefore, the needed composite properties dictate the fiber and matrix properties. Hence, selecting the composite involves selecting the best combination of fiber and matrix alloys.

Since the composite blade will be built up using separate plys that can differ in composition (to be described later), the TFRS composition need not be constant from blade tip to blade root. A particular fiber-matrix combination can be picked to best serve in the airfoil, while a different combination can be used in the root. Generally, the airfoil requirements are most severe. Consequently, this paper gives primary attention to an airfoil composition.

In the light of general blade airfoil requirements, specific composite fiber and matrix requirements are as follows.

Fiber Property Requirements

Creep-rupture strength must be adequate to permit a 50 K composite blade metal temperature advantage over current superalloys.

Mechanical fatigue strength must be adequate to permit a 50 K temperature advantage over current superalloys.

Toughness must be adequate at operating temperature to insure the needed foreign object damage (FOD) resistance.

Cost must be low so that blade fabrication costs can be kept acceptably low.

Matrix Property Requirements

Oxidation and hot corrosion resistance will be needed in the matrix at temperatures up to 1420 K. Not only is this a severe temperature in general, but the fibers lack oxidation resistance and must be protected by the matrix.

Compatibility with the fibers is required at fabrication and operating temperatures so that fiber strength is not excessively degraded by interdiffusion.

Mechanical and thermal fatigue resistance is needed at operating temperatures. Thermal fatigue damage in the matrix can be initiated by the thermal expansion coefficient mismatch between fiber and matrix (as well as by large temperature gradients).

Density must be low to help offset the high density (19000 kg/m^3) of the tungsten fibers. This is a particularly important consideration in aircraft engines where weight must be minimized because high blade densities can lead to high disk weights.

Toughness and ductility must be high at low temperatures because the matrix imparts impact damage resistance to the composite at low temperatures.

Shear creep strength must be adequate to allow fiber angle plying for airfoil chordwise strength and torsional strength.

TUNGSTEN/FeCrAlY COMPOSITE PROPERTIES

A review of the literature, presented in this section, indicates that a thoriated tungsten fiber reinforced FeCrAlY matrix composite (W/FeCrAlY) would be most likely to meet the stated requirements. As already mentioned, some composite properties are fiber controlled and others are matrix controlled. Consequently, it may aid understanding to group the expected composite properties according to fiber control, matrix control, or both. This is done in the following sections. Note that complete composite data were not available for W/FeCrAlY; therefore, the authors predicted some properties using the properties of other TFRS as a guide. Also, note that a particular fiber alloy W-1 percent ThO_2 (W-1 ThO_2) and matrix alloy Fe-24 Cr-5 Al-1 Y (FeCrAlY) are described in detail; however, these exact elemental compositions are not rigid choices and may be modified to improve W/FeCrAlY properties.

Fiber Controlled Properties

The fibers provide strength and high temperature foreign object damage (FOD) resistance to the composite. Tungsten fibers, dispersion strengthened with thoria or hafnium carbide, have adequate strength for turbine blades (ref. 11). Unfortunately, the strongest of these fibers are currently produced in laboratory quantities at high cost. Thus, W-1 ThO_2 lamp filament wire was selected as a first generation fiber based primarily on availability and low cost. The modest strength of currently produced W-1 ThO_2 wire seems adequate (as will be shown), and improvement may be possible because the thermal mechanical processing has not been optimized for 1000 to 1400 K strength. The following describes the fiber controlled composite properties that can be expected when using this fiber.

Creep resistance - Creep data for unidirectionally reinforced 45 volume percent W-1 ThO_2/FeCrAlY have been obtained at 1310, 1370, and 1420 K (ref. 8). Figure 2 is a plot of total creep strain versus time for the composite and a DS eutectic. Note that the composite specimens tested at 1370 and 1420 K had their stresses step increased during the test; because of this step loading, it is difficult to identify a well defined minimum creep rate. However, visual comparison of the composite creep curves with those of the DS eutectic indicates a potential composite use-temperature advantage greater than the desired 50 K. In other words, the figure indicates that the creep behavior of the TFRS at 1370 K is similar to that of the DS eutectic at 1310 K.

Rupture strength - Stress to cause rupture data have also been obtained for uniaxially reinforced 30- and 45-volume-percent W-1 ThO_2/FeCrAlY at 1310, 1370, and 1420 K (ref. 8). Figure 3 is a Larson-Miller plot of the rupture stress divided by density for the 45 volume percent composite, a DS eutectic, an oxide dispersion strengthened superalloy (ODSS), and a DS superalloy. The potential use-temperature of the composite is greater than those of the other three materials, and it exceeds that of the DS superalloy and DS eutectic by the desired 50 K.

High cycle fatigue resistance - High cycle fatigue tests have not been conducted on W-1 ThO_2/FeCrAlY. However, they have been conducted on W-1 ThO_2/Hastelloy X (ref. 4). Fatigue tests were performed at 10 to 15 Hz using direct stress, tension-tension, axially loaded specimens. The specimens were cycled from a minimum stress to a selected maximum stress and back to the minimum stress. The load ratio, R, ranged from 0.1 to 0.7 for unreinforced Hastelloy X and 0.1 to 0.2 for the composite. The composite load ratios represented a more severe test. Test temperatures were room temperature, 1090, 1170, and 1255 K. Composite specimens were unidirectionally reinforced and contained 23, 30, and 37 volume percent fibers. The stress to cause failure in 1×10^6 cycles versus temperature is plotted in figure 4. Unreinforced Hastelloy X data are plotted for comparison. The composite was stronger at all temperatures, ranging from 1.2 times as strong at room temperature to 4 times as strong at 1255 K. The ratio of fatigue strength to ultimate tensile strength is plotted in figure 5 for both materials. For all test temperatures, this ratio for the composite was higher than that for the Hastelloy X. This indicates that composite high cycle fatigue resistance is controlled by the fiber. Based on this result, it is expected that W-1 ThO_2/FeCrAlY also would have high cycle fatigue strength sufficient for turbine blades. Push/pull and reverse bend fatigue strength data were presented for a W/superalloy composite in reference 12; the results were similar to the forgoing.

Matrix Controlled Properties

Matrix controlled properties are many, but no matrix alloy is perfect in every respect. Thus, the major task in composite selection is selecting a matrix that provides the best compromise with respect to the needed properties. The generic alloy FeCrAlY seems to offer the best compromise at this time. The following will describe the composite properties expected using a FeCrAlY alloy as the matrix.

Oxidation and corrosion resistance - The oxidation and corrosion resistance of W-1 ThO_2/FeCrAlY composites with completely matrix encased fibers is dependent on the FeCrAlY matrix. Alloys based on the ternary Fe-Cr-Al with yittrium additions are among the most oxidation resistant alloys known. As a result, they are used on DS eutectics and superalloys as oxidation resistant coatings. Therefore, the composite with a FeCrAlY matrix should have adequate oxidation and corrosion resistance.

As examples of the oxidation and corrosion resistance possible with FeCrAlY, the following data should be noted. High gas velocity cyclic tests for oxidation at 1370 K and hot corrosion at 1170 K have been run using FeCrAlY and other alloys (ref. 13). The FeCrAlY was unsurpassed in oxidation resistance and better in hot corrosion resistance than the other materials. Figure 6 is a plot of Mach 0.3 burner rig cyclic oxidation data for FeCrAlY and NiCrAlY specimens (each cycle was 1 hr at 1370 K followed by 180 s of forced air cooling). Both materials had excellent oxidation resistance. Figure 7 is a similar plot for FeCrAlY, NiCrAlY, and IN-792 using the same test conditions with these exceptions: the temperature was 1170 K, and 5 ppm synthetic sea salt was added to the combustion products. This test measures hot corrosion resistance and is an accelerated test. IN-792 is considered to have good hot corrosion resistance, but it suffered a drastic weight loss, which indicated a severely curtailed useful life, after only 150 hours exposure. On the other hand, FeCrAlY showed no indication of weight loss after 2313 hours and had much better hot corrosion resistance than NiCrAlY.

Limited static air oxidation data for W-1 ThO_2/FeCrAlY is in agreement with the forgoing cyclic tests (ref. 8). Composite samples with completely matrix protected fibers were exposed to static air at 1310, 1370, and 1420 K for up to 1000 hours. The weight change in 1000 hours was 0.3 mg/cm^2 for 1310 K and 1.26 mg/cm^2 for 1420 K.

The preceding assumed that the fibers were completely protected by matrix. FOD could expose fibers to the engine gasses, and accelerated fiber oxidation would then occur. The oxidation need not be catastrophic, however, as is illustrated by what follows. Figure 8 illustrates the principal paths for oxidation and corrosion of exposed fibers. Oxidation proceeding perpendicular to the fibers (through the blade thickness) would destroy the exposed fibers, but intervening matrix would prevent oxidation of subsequent layers. Thus, only a partial loss of strength would result. Oxidation parallel to the fibers (along the blade span) potentially is more severe, since all the exposed fibers in the cross section potentially could be oxidized along their entire length. However, studies conducted to evaluate oxidation along fibers showed only limited oxidation penetration along the fibers (refs. 12 and 14). It was found that after 10 hours exposure to static air at 1480 K, the fibers in W-1 ThO_2/FeCrAlY were oxidized to a depth of only 2.5 mm. After 100 hours exposure at 1370 K, the fibers in a W/superalloy composite oxidized to a depth of 1.3 mm in static air and to 2.5 mm in a simulated engine exhaust gas stream moving at 1.8 m/s. These results indicate that a catastrophic loss of the exposed tungsten fiber did not occur upon exposure to a high-temperature oxidizing environment.

Long time fiber/matrix compatibility - The long time strength retention of the composite is primarily a function of fiber-matrix interdiffusion. Such interdiffusion can greatly reduce the strength of the fibers; so, the interdiffusion of W-1 ThO_2 with FeCrAlY has been studied (ref. 8). Specimens containing 0.38-mm-diameter fibers were heated to 1310, 1370, and 1420 K for up to 1000 hours. Table I lists the measured interdiffusion reaction zone depth in the fiber and the corresponding exposure times. At 1310 K, the reaction depth is almost nil, and at 1370 K only 10 percent of the fiber area reacted after 1000 hours. These are acceptable reaction rates that indicate potentially excellent long-time strength retention.

Thermal fatigue resistance - Thermally induced stresses are generated in turbine blades because of temperature gradients. These gradients change with time, leading to cyclic stresses and hence potential fatigue failures, particularly at stress concentrations such as cooling holes. Superimposed on these stresses, in the case of the composite, are internal stresses caused by the difference in expansion coefficient between the fibers and matrix. This is potentially the most serious limitation on composite usefulness. Consequently, much attention is being paid to improving the resistance of W/superalloy composites to damage due to thermal cycling.

The response of W-1 ThO_2/FeCrAlY to thermal cycling has been evaluated and found promising (ref. 14). Specimens containing 30 volume percent fiber were exposed to 1000 heating and cooling cycles from 300 to 1480 K. The heating rate was about 19 K/s (kelvin/second); while the cooling rate was about 4 K/s. The heating time was 60 s to 1480 K. Cooling down to 670 K was accomplished in an additional 90 s. The total heating and cooling cycle was accomplished in 300 s. Surface roughening was observed, but there was no matrix or fiber cracking apparent after the 1000 cycles. Similar studies were conducted by the present authors. Heating to 1370 K took 30 s and cooling to room temperature took 60 s, representing a more severe cycle than that of reference 14. Again, surface roughening was apparent but cracking of fiber or matrix did not occur; furthermore, the specimens were dimensionally stable.

Preliminary thermal fatigue burner rig tests were also performed on W-1 ThO_2/FeCrAlY containing 35 volume percent fiber (ref. 8). Unidirectionally reinforced composite panels having a rectangular shape were rotated at 29 revolutions per second and subjected to a flame velocity of Mach 0.5. Jet A fuel with 35 ppm synthetic sea salt and a sulfur content of 0.4 percent was used. The specimens were heated to 1370 K within 120 s and held for 240 s. Cooling consisted of exposing the specimens to an air blast for 120 s. Panels exposed to 104 cycles showed no indications of matrix or fiber damage.

Fiber-Matrix Controlled Properties

The density, elastic constants, impact resistance, and thermal conductivity are functions of both fiber and matrix properties. The following describes the anticipated values for W/FeCrAlY.

Density - Composite density can be calculated using the rule of mixtures. The density of W-1 ThO_2 wire is about 18900 kg/m^3. The density of FeCrAlY is about 7200 kg/m^3, depending on the exact elemental compositions. A typical 40-volume-percent fiber content, W/FeCrAlY composite would have a density of 11 900 kg/m^3.

Impact damage resistance - Pendulum impact tests have been conducted on W-1 ThO_2/FeCrAlY (ref. 15). Notched minature Izod specimens were tested from room temperature to 645 K. The impact values obtained are shown in figure 9. A pronounced ductile-brittle transition occurred at about 470 K. Extrapolated miniature Izod values indicate potential Charpy values of 4.1 J at room temperature and 72 J at 470 K. Similar values were reported for W/nickel alloy composites (ref. 3). Composite impact strength was shown to depend on the matrix toughness at temperatures below the ductile-brittle transition temperature (DBTT) of the fibers (about 500 K). Unfortunately, the FeCrAlY matrix used in the tests, the results of which are shown in figure 9, had a DBTT above 400 K; consequently, it could not provide the needed toughness. However, other FeCrAlY alloys have DBTTs near room temperature (ref. 16). Use of those alloys should greatly increase the room temperature impact strength of the composite.

Elastic constants - The nominal composite ply modulus in the fiber direction (E11) can be calculated using the rule of mixtures. The transverse ply modulus (E22) and shear modulus (E12) may be approximately calculated using a more involved equation (ref. 17). However, the moduli so calculated are not constants. As the composite is strained the matrix will exceed its proportional limit (but the fibers will not exceed their's). Thus, the contribution of the matrix alloy modulus changes as a function of composite strain. Consequently, the stress-strain relationship on unloading will be different from the relationship on loading. Therefore, W/FeCrAlY stress analyses using linear elastic methods (as most-finite element analyses presently do) can only be considered as being approximate. For approximation purposes, the fiber modulus is 380 GPa at 1050 K and 360 GPa at 1350 K. The matrix modulus is about 140 GPa at 1050 K and 100 GPa at 1350 K. Poissons ratio is about 0.29 for the fiber and about 0.30 for the matrix below its proportional limit.

Thermal conductivity - High thermal conductivity is desirable in a turbine blade material to reduce temperature gradients; this, in turn, results in reduced thermally induced strains that can cause cracks or distortion. In addition, higher conductivity can reduce coolant flow requirements in some impingement cooled blades leading to greater engine efficiency or durability (ref. 9). The conductivity of W/FeCrAlY will be high because the conductivity of tungsten is high (the conductivity of FeCrAlY is similar to that of other superalloys) (ref. 9). Thermal conductivity of the composite is greatest in the direction of the fiber axes since there is a continuous path for conduction along the tungsten fibers. Conduction perpendicular to the fiber axes is lower because the heat cannot find a continuous path through tungsten. W-1 ThO_2/FeCrAlY conductivity has been measured for some fiber contents and temperatures and extrapolated to other conditions as shown in figure 10 (ref. 9). The extrapolation indicates that at blade conditions (30 to 60 volume percent fibers and 1000 to 1400 K) the transverse (through the wall) conductivity of the composite will be 35 to 50 W/m-K. The longitudinal (spanwise) conductivity will be about 45 to 65 W/m-K (ref. 9). Typical superalloys have conductivities of about 25 W/m-K at 1300 K.

TUNGSTEN/FeCrAlY BLADE FABRICATION AND COST

The material properties reviewed in this paper and reported in references 8, 9, 14, and 15 on laboratory specimens indicate that W/FeCrAlY composites have the properties needed in turbine blades. Having demonstrated adequate properties, the next area of consideration is whether complex blades can be designed and fabricated from such a composite at reasonable cost. The following discusses these considerations as they apply to hollow W/FeCrAlY turbine blades.

Investment casting has been considered for fabrication of hollow composite blades; however, there are two obstacles to overcome. A way must be found to hold the fibers in positive 'angle plied' alignment during infiltration by the molten matrix. Also, small diameter fibers must be used in hollow blades because of a space limitation and these fibers are subject to damage caused by fiber-matrix interdiffusion. Therefore, either fibers must be coated to resist fiber-matrix interdiffusion during infiltration (no effective coating currently exists) or casting and cooling must take place quickly to limit interdiffusion. We feel that, given the current state of the art, investment casting would be most successful in fabrication of uniaxially reinforced solid blades in which large fibers can be used.

Diffusion bonding of monolayer composite plies is currently the most promising, cost effective method of fabrication for a hollow blade. The composite plies would consist of aligned tungsten fibers sandwiched between layers of FeCrAlY. This approach has the capability for accurate fiber distribution and alignment; moreover, it limits fiber-matrix interdiffusion during fabrication. This approach should also be capable of producing blade shapes that would be close to final dimensions; hence, only root machining and touch up grinding would be needed. This approach has been used to fabricate solid B/Al and Ti fan and compressor blades. Higher bonding temperatures than those used for Al and Ti matrix composites will be needed for the W/FeCrAlY, and a method to produce a hollow blade must be developed. But no other major differences are expected to complicate fabrication.

Figure 11 shows the sequence used to fabricate B/Al fan blades; this sequence is similar to the one anticipated for W/FeCrAlY fabrication. Large B/Al monotape sheets are first fabricated. These sheets are then cut into the plies necessary to arrive at the final blade dimensions. Many plies are cut from a sheet resulting in little scrap loss. The plies are then stacked in a shuttle box containing positioning ribs to insure accurate alignment. The box is placed in a preheated press, and pressure is applied. The result is an as-pressed blade of near finish dimensions.

The blade fabrication process requires that the composite material be available in monotape form. Past NASA contracts have resulted in developing a process to successfully fabricate TFRS material in monotape form (refs. 18 and 19). The fabrication sequence used to produce monotape of this material is shown in figure 12. The superalloy matrix material is used in sheet form, if available. Alternatively, matrix alloy powder can be made into sheets of powder cloth. Powder cloth is made by blending the powder with teflon, and then rolling it to the desired thickness. Fiber mats are made by winding the fibers on a drum, and then spraying them with a binder. The fiber array is cut from the drum and flattened to form a fiber mat. The fiber mat is then placed between two sheets of powder cloth or alloy sheet, encapsulated, and diffusion bonded in a press or between rollers. Before bonding, the binders are completely removed by evaporation during the heating process which is done in vacuum.

The special concepts evolved to fabricate hollow blades are shown in figure 13(a). The same technique used to fabricate solid blades would be used to fabricate a hollow blade with two exceptions. The plies would be pressed around a leachable core material, and plies would be wrapped around the leading edge of the blade. A superalloy root would be bonded to the composite airfoil. The core material would then be leached out with acid and an endcap would be bonded to the tip of the airfoil. If complex cooling passages are required, and impingement cooling insert containing these passages would be placed in the leached out cavity and brazed to the root of the blade. Figure 13(b) provides a schematic illustration of how cooling exit holes could be produced as well as another concept for hollow blade fabrication. The required plies would be formed having fiber free areas where cooling holes would be located. The plies would be X-rayed, and the required holes would be drilled. The plies would then be formed around a leachable core mandrel and welded along the trailing edge. This assembly could then be pressed in a die to arrive at the proper airfoil contour. Afterwards, the core material would be leached out, root and end cap bonded in place, and an insert placed in the hollow cavity if desired.

The complete fabrication sequence incorporating the concepts presented is shown in figure 14. This fabrication sequence was used in a fabrication cost study (ref. 20). Fabrication costs were estimated for high technology turbine blades fabricated using three different materials. The same turbine blade configuration, a first stage JT9D blade, was used for each material. Directionally solidified eutectic (DSE), an oxide dispersion strengthened superalloy (ODSS), and W/FeCrAlY blade manufacturing costs were compared with the cost of producing the same blade from a DS superalloy. The relative costs are shown in figure 15. The study indicates that W/FeCrAlY manufacturing costs should be competitive with current manufacturing costs of manufacturing this blade by directional solidification of a superalloy.

PRELIMINARY TUNGSTEN/FeCrAlY BLADE DESIGN

Because W/FeCrAlY has potentially excellent properties and because projected blade manufacturing costs look attractive, NASA decided to investigate the fabrication of W/FeCrAlY turbine blades. And, at this writing, such an effort is being made contractually. In support of this effort, a blade was designed by NASA to allow demonstration of several fabrication concepts. The factors considered in this design are outlined below.

Rather than use an arbitrary geometry, a JT9D first stage, convection cooled blade was selected (fig. 16). There were several reasons for this. The JT9D blade is a relatively low stress, high temperature blade. This permits more efficient use of the composite's strength versus temperature properties. It has a relatively long airfoil with little twist which makes it easier to design and fabricate. It is currently flying in many aircraft; so an improved version may have near term value. And, it is the blade the comparative fabrication cost of which was estimated in reference 20. Therefore, its fabrication would provide a check on the validity of those cost estimates.

A major purpose of the blade fabrication contractual effort is to demonstrate that design requirements can be met in the fabricated blade. To that end, a concerted effort is being made to incorporate a number of design concepts into the blade at the expense of fabrication ease. Among these are the following concepts:

Based on the forgoing, the authors feel that W/FeCrAlY is the correct TFRS to begin the transition from laboratory data to rig testable hardware. However, a great deal of work remains to be done in the practical matters of fabrication and design. Current efforts at the NASA Lewis Research Center and in industry are addressing problems in those areas.

Although W/FeCrAlY is a promising TFRS, it should be borne in mind that it is a first generation TFRS. Much stronger fibers (than W-1 ThO_2) have been identified. Similarly, matrix alloys offering potential improvements over FeCrAlY have been studied in our research. Unfortunately, these improved materials are currently produced only on a laboratory scale and in quantities too small for the needs of an agressive development program. However, with effort these materials could be made available in required quantities at low cost. Such a program will be undertaken eventually. Consequently, the true potential of TFRS is much greater than that of W/FeCrAlY.

REFERENCES

1. Bibring, H: High Temperature Problems In Gas Turbine Engines, AGARD Conference No. 229, p. 20-1, Middle East Technical University, Ankara, Turkey, Sept. 19-23, 1977.

2. Petrasek, D. W. and Signorelli, R. A.: NASA TN D-7773, Washington, D.C., 1974.

3. Winsa, E. A. and Petrasek, D. W.: NASA TN D-7393, Washington, D.C., 1973.

4. Baskey, R. H.: AFML-TR-67-196, Air Force Materials Lab., Wright-Patterson, Ohio, 1967.

5. Morris, A. W. H. and Burwood-Smith, A.: Fibre Sci Technol., 1970, vol. 3, p. 53.

6. Glenny, R. J. E.: Proc. Roy. Soc. (London), Ser. A, 1970, vol. 319, p. 33.

7. Kotov, V. F., Fonshtein, N. M., and Shvarts, V. I.: Metalloved. Term. Obrab. Metal., 1971, no. 8, p. 20.

8. Brentnall, W. D.: TRW-ER-7790-F, TRW, Inc., Cleveland, Ohio, 1976 and Noval Air Development Center, Warminster, Penn., 1976.

9. Winsa, E. A., Westfall, L. J., and Petrasek, D. W.: NASA TM-73842, Washington, D.C., 1978.

10. Sheffler, K. D. and Jackson, J. J.: PWA-5472, Pratt & Whitney Aircraft, East Hartford, Conn., 1976. also NASA CR-135005, Washington, D.C., 1976.

11. Petrasek, D. W.: NASA TN D-6681, Washington. D.C., 1972.

12. Dean, A. V.: NGTE-R-266, National Gas Turbine Establishment, Pyestock, England, 1965.

13. Lowell, C. E. and Deadmore, D. L.: NASA TM X-73656, Washington, D.C., 1977.

14. Brentnall, W. D., Moracz, D. J., and Toth, I. J.: TRW-ER-7722-F, TRW, Inc., Cleveland, Ohio, 1975.

15. Brentnall, W. D.: TRW-ER-7887-F, TRW, Inc., Cleveland, Ohio, 1977 and NADC 76077-30, Naval Air Development Center, Warminster, Penn., 1977.

16. Wukusick, C. S.: GEMP-414, General Electric Co., Cincinnati, Ohio, 1966.

17. Ashton, J. E., Halpin, J. C., and Petit, P. H.: Primer on Composite Materials: Analysis. Progress in Materials Science Series, Vol. 3, Technomic Publishing Co., Inc., Westport, Conn., 1969.

18. Brentnall, W. D. and Toth, I. J.: ER-7757, TRW Equipment Labs., Cleveland, Ohio, 1974 and NASA CR-134664, Washington, D.C., 1974.

19. Brentnall, W. D. and Moracz, D. J.: ER-7849, TRW, Inc., Cleveland, Ohio, 1976 and NASA CR-135021, Washington, D.C., 1976.

20. Barth, C. F., Blake, D. E., and Stelson, T. S.: TRW-ER-7930, TRW, Inc., Cleveland, Ohio, 1977 and NASA CR-135203, Washington, D.C., 1977.

TABLE I. - THERMAL STABILITY OF FeCrAlY COMPOSITE

[0.038-cm (0.015-in.) diameter W-1% ThO_2 fiber.]

Exposure			*Reduction in fiber area, %	*Reaction zone width	
Temperature		Time hrs.		cm	in.
°K	°F				
1310	1900	10	<0.5	0.36×10^{-3}	0.14×10^{-3}
		100	<0.5	.38	.15
		1000	<0.5	.89	.35
1370	2000	10	<0.5	.30	.12
		100	<0.5	.66	.26
		1000	9.5	1.78	.70
1420	2100	10	<0.5	.41	.16
		100	0.88	1.17	.46
		1000	16.10	3.20	1.26

*From ref. 8

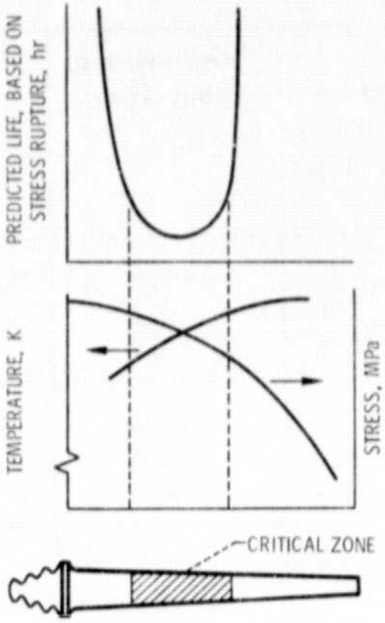

Figure 1. - Critical zone of turbine buckets.

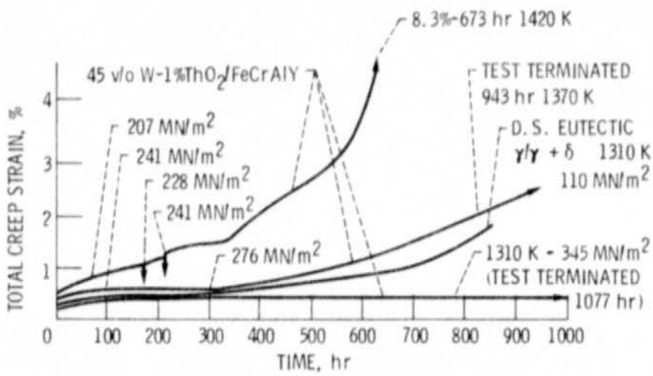

Figure 2. - Comparative creep data for W-1%ThO_2/FeCrAlY and DS eutectics (ref. 8).

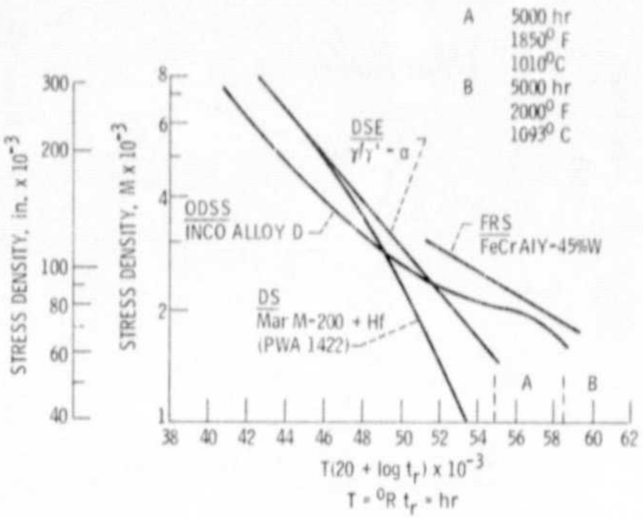

Figure 3. - Comparative (density-normalized) Larson-Miller stress-rupture curves (longitudinal properties) for advanced turbine blade materials (ref. 20).

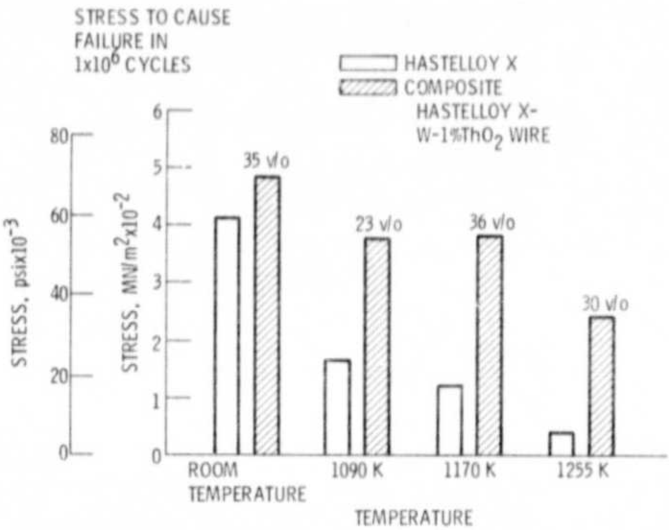

Figure 4. - Stress for failure in $1x10^6$ cycles for Hastelloy X and composite tested in axial tension-tension (ref. 4).

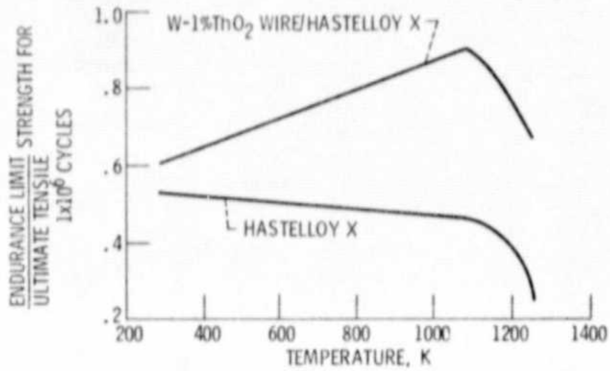

Figure 5. - Ratio of endurance limit to ultimate tensile strength for Hastelloy X and composite tested in axial tension-tension (ref. 4).

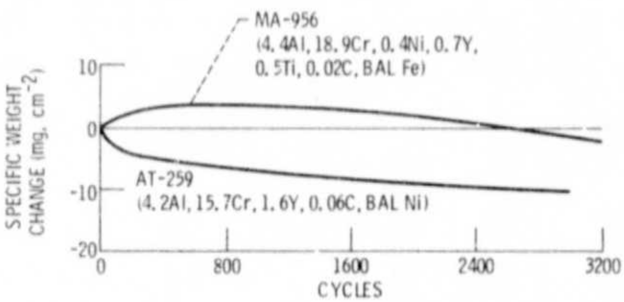

Figure 6. - Mo. 3 cyclic oxidation of some oxide dispersion strengthened alloys at 1373 K. One hour at temperature per cycle, forced air cooled for 180 seconds (ref. 13).

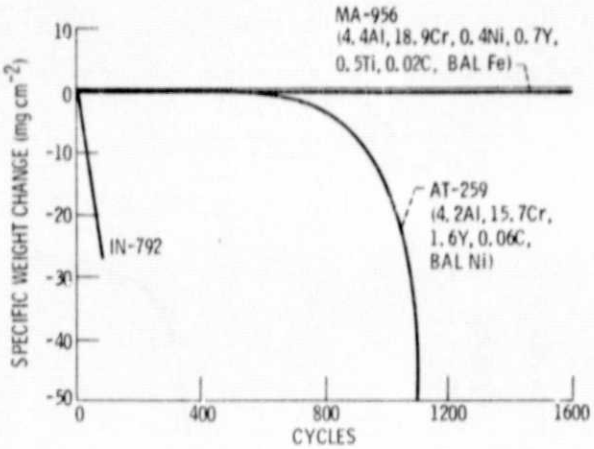

Figure 7. - Hot corrosion of some oxide dispersion strengthened alloys as compared to a typical Ni-base superalloy. One hour at 1273 K per cycle, forced air cooled 180 seconds, 5 ppm synthetic sea salt (ref. 13).

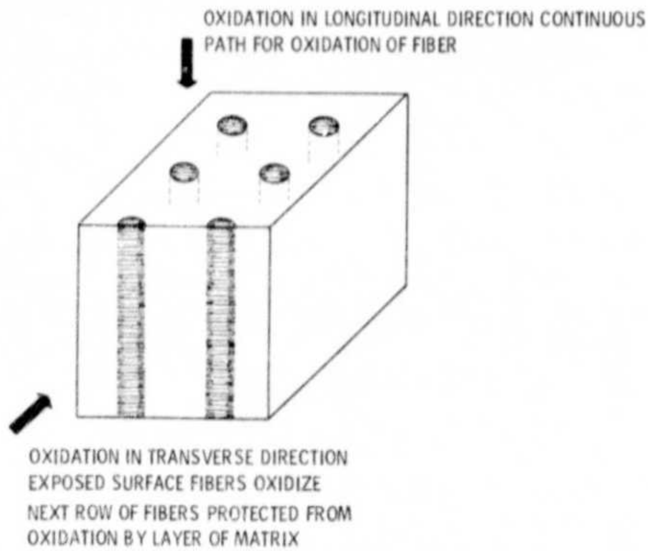

Figure 8. - Principal paths for exposed fiber oxidation.

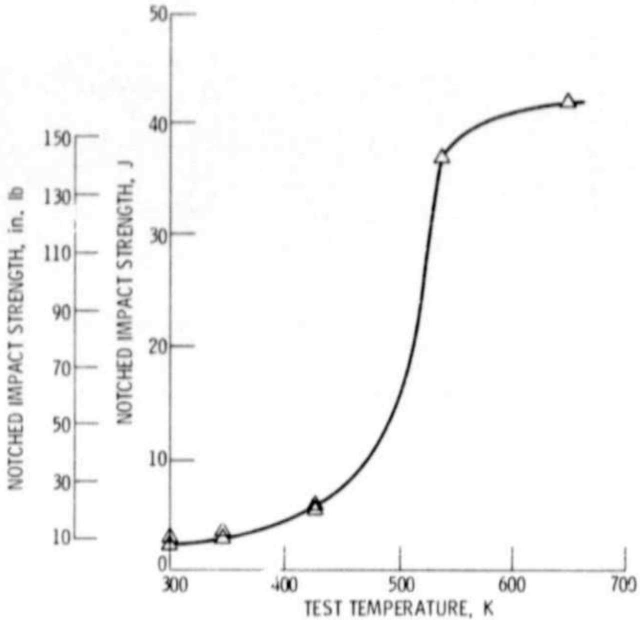

Figure 9. - Miniature Izod notched impact strength vs temperature for W/FeCrAlY composites (ref. 15).

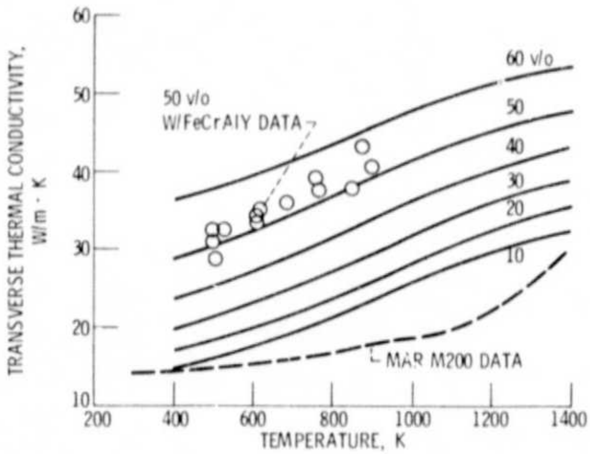

Figure 10. - Calculated transverse (through the wall) conductivities of typical TFRS (ref. 9).

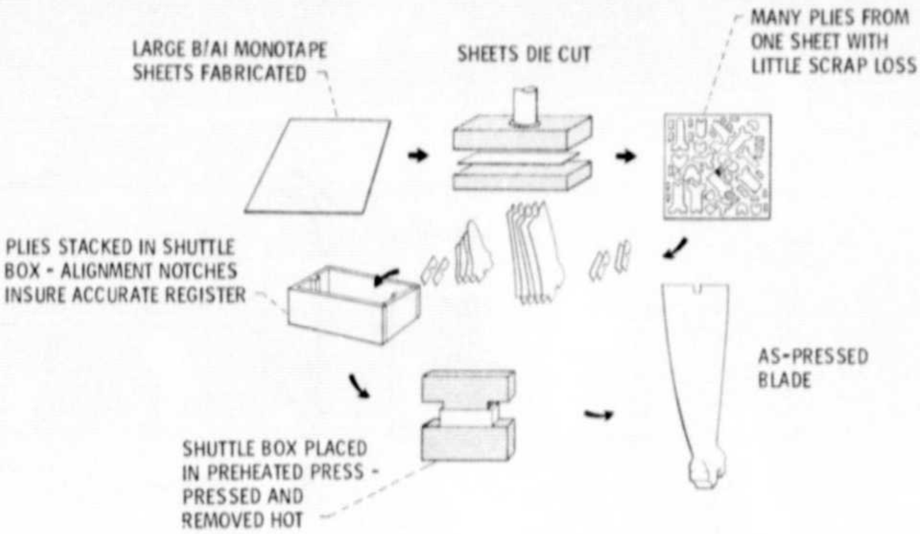

Figure 11. - Boron/aluminum fan blade fabrication sequence.

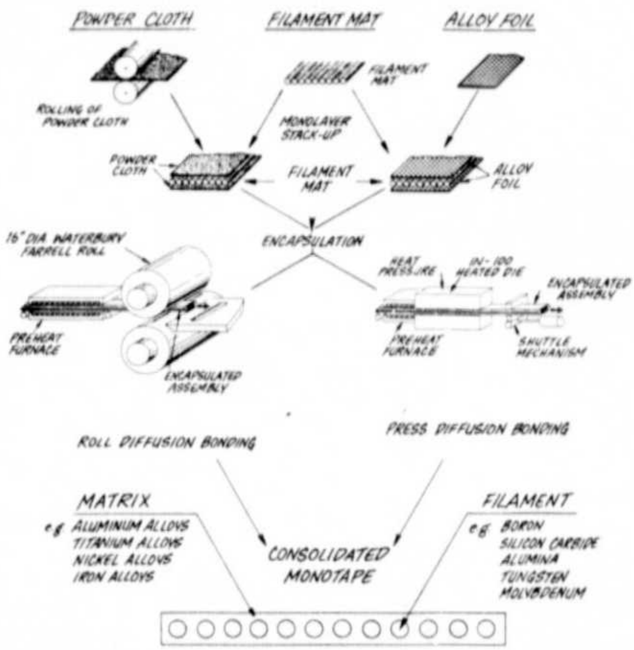

Figure 12. - Manufacture of filamentary metal matrix composite monotapes.

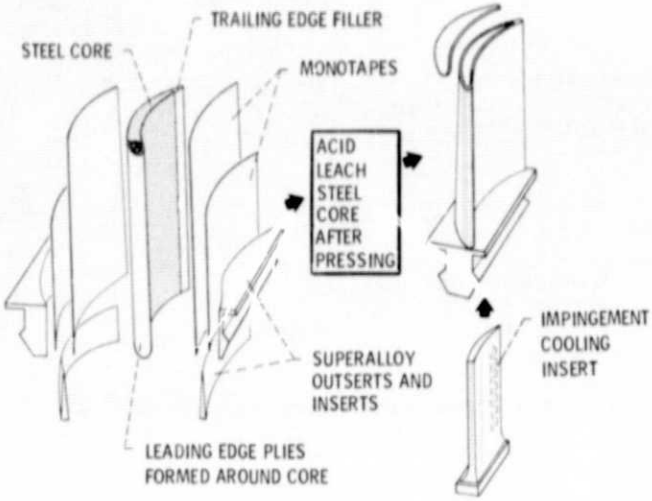

(a) DIFFUSION BONDED OUT PLIES.

Figure 13. - Hollow blade fabrication concepts.

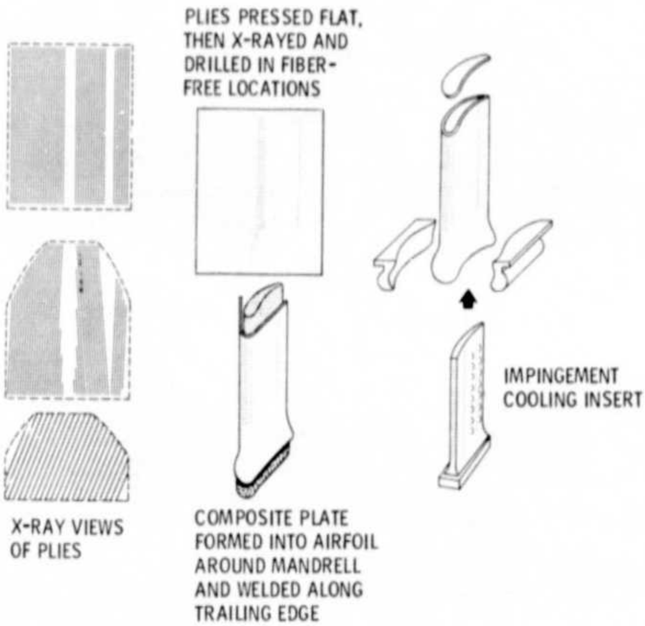

(b) WRAPAROUND FORMED PLIES.

Figure 13. - Concluded.

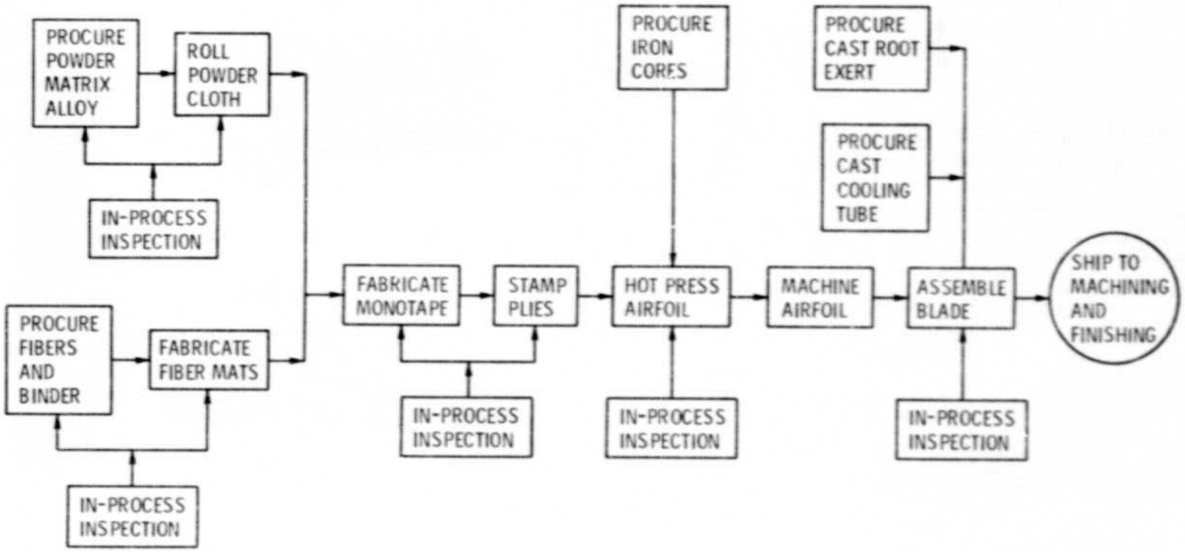

Figure 14. - Fabrication sequence for FRS turbine blades.

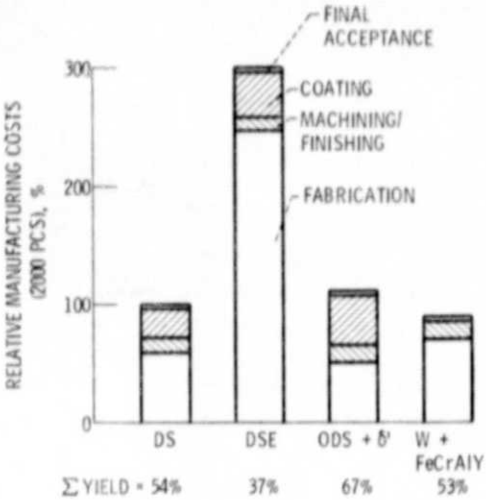

Figure 15. - Cost analysis for JT9D first stage turbine blade (ref. 20).

Figure 16. - First stage JT9D turbine blade.

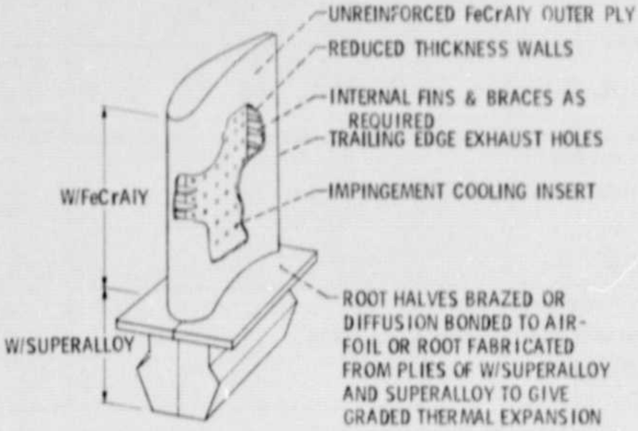

Figure 17. - Schematic of FRS JT9D blade designed for fabrication feasibility experiments.

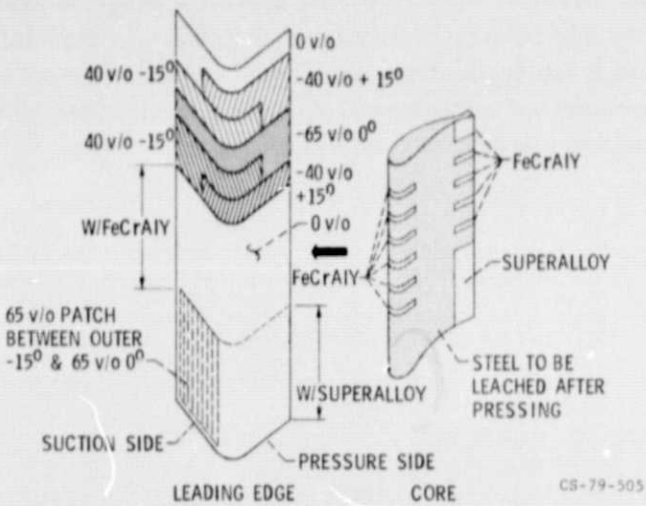

Figure 18. - Schematic of airfoil ply configuration in JT9D blade.